

Dose-dependent modulation of choroidal neovascularization by plasminogen activator inhibitor type I



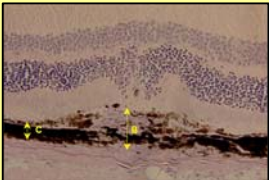
Lambert V^{1*}, Munaut C^{1*}, Bajjou K^{1*}, Carmeliet P², Gerard R³, Declerck P⁴, Gils A⁴, Claes C⁵, Foidart J.-M.^{1*}, Rakic J.-M⁶ and Noël A^{1*}

¹Laboratory of Tumor and Development Biology, ULg, ²Center for Transgene and Gene Therapy, KUL, ³Departments of Internal Medicine and Molecular Biology, University of Texas Southwestern Medical Center, Texas, USA, ⁴Pharmaceutical and Phytopharmacology, KUL, ⁵Department of Ophthalmology, Middelheim Hospital, Antwerpen, ⁶Department of Ophthalmology, ULg, BELGIUM. *Center of Experimental Cancer Research (CRCE), ULg, BELGIUM.

A- ABSTRACT

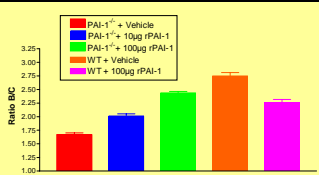
Pathological neovascularization growing from the choroid under the retina is the most severe form of age-related macular degeneration (AMD). Plasminogen activator inhibitor type 1 (PAI-1) is believed to control proteolytic activity and cell migration during angiogenesis, and we have shown previously that this inhibitor was necessary for the development of murine laser-induced choroidal neovascularization (Lambert et al. FASEB J 2001). We report here that PAI-1 expression is induced in the course of both human and experimental choroidal neovascularization. Daily injection of recombinant PAI-1 proteins in controls and PAI-1 deficient animals proved that PAI-1 could exert a proangiogenic effect at low doses and an antiangiogenic effect at high levels. Using specific PAI-1 mutants to further dissect the mechanisms of PAI-1 effect in this model, we show that PAI-1 promotes choroidal pathological angiogenesis merely through its antiproteolytic activity but also in part through its interaction with vitronectin.

Quantification of neovascularization.



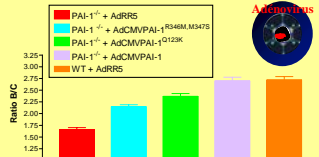
B = the thickness from the bottom of the choroid to the top of the neovascular area.
C = thickness of intact adjacent choroid.

Dose-dependent effect of recombinant PAI-1 on choroidal neovascularization.

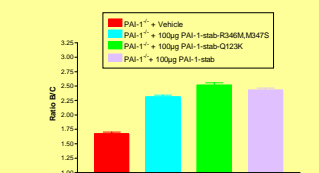


We demonstrate dose dependent pro- or antiangiogenic effect of rPAI-1.

Molecular mechanism by which PAI-1 promotes choroidal angiogenesis.



Infection of PAI-1 deficient mice with AdCMVPAI-1^{Q123K} partly restored (80%) the amount of CNV observed in WT mice infected with control AdRR5 or in PAI-1^{-/-} animals infected with AdCMVPAI-1, but more efficiently than in the case of infection with AdCMVPAI-1^{R346M,M347S} (67%).



PAI-1^{-/-} mice were, in a separate experiment, daily injected with an identical dose of recombinant PAI-1 variants (100 µg/ml) harbouring the same mutations as those present in the adenoviral constructs.

B- MATERIALS AND METHODS

RT-PCR analysis of human neovascular membranes

The methods conform to the Declaration of Helsinki for research involving human subjects. Eight consecutive submacular CNV specimens were completely removed during surgery for 360° macular translocation performed on exudative AMD patients (3 male, 5 female, mean age 77 yrs, range 72-83) either not amenable to conventional laser/photodynamic therapy (presence of occult neovessels or submacular bleeding) or for one patient, due to a large recurrence occurring a few months after a successful medical treatment. The specimens were immediately frozen in liquid nitrogen and stored at -80°C.

Laser pressure catapulting (LPC) and RT-PCR

8 to 10 serial frozen sections were mounted directly onto a 1.35 m thin polyethylene foil (PALM, Wolfratshausen, Germany). The supporting membrane was mounted onto the glass slide using the Microbeam-MOMENT technique¹⁵. The membrane-covered slides were stored at room temperature until needed. The Robot-Microbeam (PALM[®]) focused the laser (337 nm) on the specimen with appropriate energy settings enabling the catapulting of the entire selected area into the microfuge cap. The entire subretinal choroidal neovascularization area (indicated below) and an adjacent intact chorioretinal zone (control) were microdissected separately on frozen sections (10 µm thick) at selected intervals after laser burn (day 3, 5, 14 and 40). The specimens were covered with 100 µl lysis buffer and total RNA isolation was performed with the PureScript RNA-isolation Kit (Biozym, Landgraf, The Netherlands) according to the manufacturer's protocol. Total RNA was dissolved in a 10 µl RNA hydration solution supplied by the manufacturer. 28S rRNA were amplified with an aliquot of 1 µl of total RNA using the GeneAmp[®] ThermoStable RT reverse transcriptase RNA PCR kit (Perkin Elmer) and two pairs of primers (Gibco BRL Life Technologies): sense: 5'-GTGACCCACTAATAGGAACGTGA-3' and reverse: 5'-GGATTCTGACTAGAGCGCTCAGT-3' for 28S mRNA, sense: 5'-AGGGCTTCATGCCCACTTCTTCA-3' and reverse: 5'-AGTAGAGGGCCATCCACCAGACCA-3' for PAI-1. Reverse transcription was performed at 70°C for 15 min followed by 2 min incubation at 95°C for denaturation of RNA-DNA heteroduplexes. Amplification started by 15 sec at 94°C, 20 sec at 68°C and 10 sec at 72°C for PAI-1 and 28S (33 cycles for PAI-1 and 19 cycles for 28S for human neovascular membranes, 45 cycles for PAI-1 and 35 cycles for 28S for LPC material). RT-PCR products were resolved on 10% acrylamide gels and analysed using a Fluor-S Multimager (BioRad) after staining with Gelstar (FMC BioProducts) dye. The expected size for RT-PCR products was 212 bp for 28S and 197 bp for PAI-1 respectively.

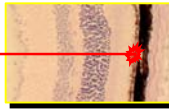
Immunohistochemistry

Cryostat sections (5µm thick) were fixed in paraformaldehyde 1% in 0.07M phosphate buffered saline (PBS) pH 7.0 for 5 min or in acetone for 10 min at room temperature and then incubated with the primary antibody. Antibodies raised against type IV collagen (guinea pig polyclonal antibody produced in our laboratory; diluted 1/100), and human Von Willebrand factor (Dako, Glostrup, Denmark; rabbit polyclonal antibody; diluted 1/200) were incubated for 1 hr at room temperature. The sections were washed in PBS (X 10 min) and appropriate secondary antibody biotinylated or conjugated to tetramethylrhodamine isothiocyanate (TRITC) added: goat anti-rabbit IgG (Dako; diluted 1/400), monoclonal anti-guinea pig IgG (Sigma; diluted 1/40) were applied for 30 min. WVI was detected with horseradish peroxidase-labeled streptavidin according to the manufacturer (DAKO) and developed with the chromogen 3,3'-diaminobenzidine tetrahydrochloride (Sigma) for 4 min. Mayer's hematoxylin was used as a counterstain. For immunofluorescence staining of ocular sections, after 3 washes in PBS for 10 min each and a final rinse in 10 mM Tris-HCl buffer, pH 8.8, labelling was analysed under an inverted microscope equipped with epifluorescence optics. Specificity of staining was assessed by substitution of nonimmune serum for primary antibody.

Adenovirus-mediated PAI-1 cDNA transfer

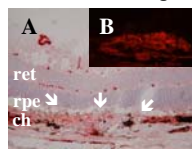
PAI-1 with the Q123K mutation had a specific 40-fold decrease in affinity for vitronectin but retained full inhibitory activity. The double point mutant, Arg 346 to Met and Met 347 to Ser²³ mutation had the same affinity as WT PAI-1 but did not inhibit PA activity. One day after choroidal neovascularization induction by laser, mice were intravenously injected with 200 µl of control or recombinant adenovirus (7 x 10⁸ PFU) encoding human PAI-1 (WT or mutants). The efficiency of transduction was evaluated with ELISA measurement of circulating PAI-1 levels and injection of adenoviruses encoding E. Coli β-galactosidase as previously described²⁰. On day 14, mice were killed and eyes were excised and processed (see above). According to regulatory constraints, the virally infected animals were permanently housed under BL3 containment and consequently fluorescein angiograms could not be performed.

MODEL OF CHOROIDAL VASCULARIZATION: Green Argon Laser Impacts.



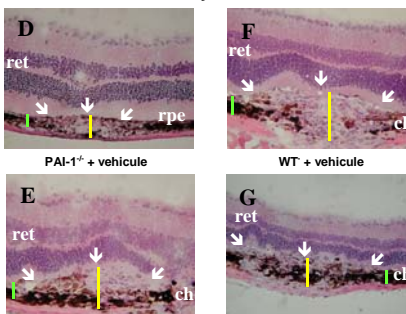
532 nm
50 µm Ø
0.05 sec
400mW

Immunostaining



A: vWf antibody; B: Coll. IV

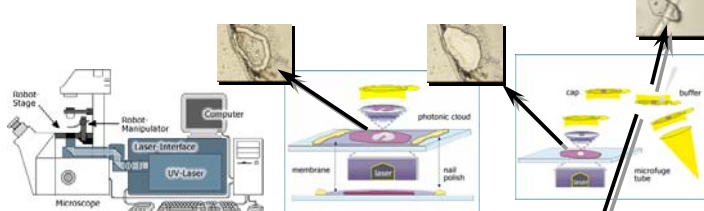
Hematoxylin/Eosin



Negative control PAI-1^{-/-} + 100µg r PAI-1 WT + 100µg r PAI-1

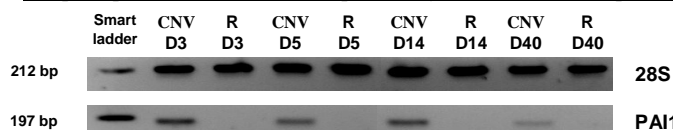
When mice were daily injected with increasing concentrations of active recombinant PAI-1 (PAI-1-stab, 10 or 100 µg/d), a dose-response effect was obtained with the higher dose nearly restoring the WT pattern. In contrast, an inhibitory effect on CNV development was observed when WT mice were treated with high dose of rPAI-1

Microdissection by Laser Pressure Catapulting (LPC).



Microdissection around the laser burn on frozen section of 8µm thickness.

Temporal pattern of PAI-1 mRNA expression by RT-PCR from LPC product.



Upregulation of PAI-1 mRNA expression is observed in WT mice at all time endpoints studied. The retinal specimens microdissected from the neighbouring intact chorioretinal areas were negative for PAI-1 mRNA throughout the study period.

I: Impact zone; C: retinal Control zone; D: Day

C- CONCLUSIONS

PAI-1 mRNA is specifically expressed in CNV both in human exudative AMD and in new vessels occurring under the retina after laser-induced trauma of the Bruch's membrane.

We provide clear evidence for dose-dependent opposite effects of PAI-1 during CNV development. The pro-angiogenic effect of PAI-1 at low concentration and its anti-angiogenic action at high concentrations are supported by the facts that:

- (1) CNV formation was inhibited in PAI-1 deficient mice;
- (2) CNV formation was restored in PAI-1^{-/-} mice by injecting rPAI-1, and the level of restoration was proportional to the injected dose;
- (3) injection of high dose of rPAI-1 (100 µg/d) into WT mice inhibited CNV development.

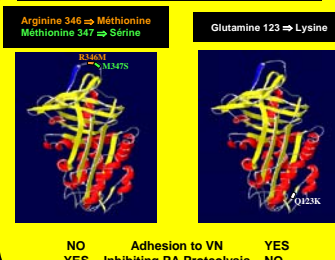
The data presented here were obtained in a model of pathological angiogenesis sharing in common at least three important features with human pathology (AMD): the presence of Bruch's membrane trauma, the choroidal origin of neovascularization and the involvement of mononuclear cells.

To separate the contribution of PAI-1 protease inhibitory activity from its vitronectin binding properties, recombinant adenoviruses expressing specific PAI-1 mutants and recombinant mutated PAI-1 proteins defective either in PA inhibition or vitronectin binding were used. These experiments didn't lead to a clear discrimination between the two mechanisms of action of PAI-1 since both mutants were able to partly restore choroidal angiogenesis when compared to PAI-1 deficient mice. However, the mutants defective in vitronectin binding restored angiogenesis in the choroid more efficiently than those unable to control PA activity.

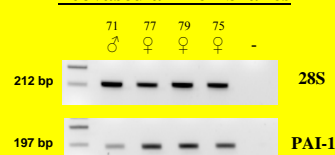
PA inhibition by PAI-1 is probably more important than vitronectin binding activity for angiogenesis promotion.

Taken together with our previous results demonstrating the necessity of PAI-1 presence for the development of experimental CNV, our findings suggest that local variations in PAI-1 concentration may modulate the progression and recurrences of exudative AMD. Another implication of our observations is that the dose dependent effect of PAI-1 on angiogenesis warrants against uncontrolled pharmacological strategies using PAI-1 agonists/antagonists for inhibition of choroidal neovascularization.

Mutated forms of human PAI-1



PAI-1 expression profile in human neovascular membranes



PAI-1 expression was not detected in normal human posterior segment. However, PAI-1 mRNA is detected in all specimens obtained during surgery.